

Technical Attenuation Length Measurement of Plastic Scintillator Strips for the Total-Body J-PET Scanner

Łukasz Kaplon 

Abstract—The aim of the performed technical attenuation length measurement is to compare light attenuation of a few commercially available plastic scintillator strips and to select the best scintillator type for the total-body Jagiellonian Positron Emission Tomograph (J-PET) construction. Few models of plastic scintillators obtained from different manufacturers were tested. All strips had the same rectangular cross section and dimensions $6\text{ mm} \times 24\text{ mm} \times 1000\text{ mm}$ with all surfaces polished. The light attenuation length was measured by exciting the scintillator strip at different positions with an ultraviolet lamp emitting at 365 nm and reading light signal collected at one side of the strip by a silicon photodiode. Among measured plastic scintillators, EJ-200 possesses the highest technical light attenuation length and is suitable for construction of total-body J-PET scanner.

Index Terms—Jagiellonian Positron Emission Tomograph (J-PET) scanner, plastic scintillator, positron emission tomography (PET), technical attenuation length (TAL).

I. INTRODUCTION

PLASTIC scintillators are used in many applications connected to radiation detection. They are characterized by short decay time (1–3 ns) and are transparent to emitted light. Their price, about two orders of magnitude lower than inorganic crystals, allows to build big radiation detectors and medical scanners. One such device is a time-of-flight positron emission tomography (TOF-PET) scanner based on plastic scintillators named Jagiellonian Positron Emission Tomograph (J-PET) [1]. The first two prototypes of J-PET are based on rectangular plastic scintillator strips with vacuum photomultiplier tubes (PMTs) attached at both ends [2]. The first J-PET prototype with 360-mm diameter ring configuration was built out of 24 BC-420 plastic scintillators with dimensions $5\text{ mm} \times 19\text{ mm} \times 300\text{ mm}$ coupled to Hamamatsu R4998 PMTs. The second one with 850-mm diameter ring configuration consists of 192 EJ-230 plastic scintillators with dimensions $7\text{ mm} \times 19\text{ mm} \times 500\text{ mm}$ coupled to Hamamatsu R9800 PMTs.

Manuscript received March 6, 2020; revised April 28, 2020; accepted May 22, 2020. Date of publication July 29, 2020; date of current version October 16, 2020. This work was supported in part by the Polish National Center for Research and Development under Grant INNOTECH-K1/IN1/64/159174/NCBR/12, in part by the Foundation for Polish Science TEAM Program under Grant POIR.04.04.00-00-4204/17, and in part by the National Science Centre of Poland under Grant 2016/21/B/ST2/01222.

The author, on behalf of the J-PET Collaboration, is with the Faculty of Physics, Astronomy and Applied Computer Science, Jagiellonian University, 30-348 Kraków, Poland (e-mail: lukasz.kaplon@uj.edu.pl).

Color versions of one or more of the figures in this article are available online at <http://ieeexplore.ieee.org>.

Digital Object Identifier 10.1109/TNS.2020.3012043

Next-generation J-PET scanners are based on modules consisting of 500- and 1000-mm-long plastic scintillator strips with silicon photomultipliers coupled at both ends [3]. We have also added a layer of wavelength shifters (WLSs) between plastic scintillators [4] to increase J-PET scanner resolution along the strip. This J-PET scanner is a portable, lightweight, and modular version with tightly arranged scintillation strips designed for the total-body examination [5] and positronium imaging [6], [7]. We already built a portable 24-module J-PET scanner based on 312 pieces of $6\text{ mm} \times 24\text{ mm} \times 500\text{ mm}$ BC-404 plastic scintillators and 2496 Hamamatsu S13361 silicon photomultipliers. One module consists of 13 plastic scintillators and a matrix of four silicon photomultipliers ($6\text{ mm} \times 6\text{ mm}$) coupled at both ends of each scintillator. All scintillators are wrapped in 3-M Vikuiti Enhanced Specular Reflector and DuPont Kapton B black light-tight foils. Tomographic data are processed with use of a field-programmable gate array system-on-chip (FPGA SoC) platform [8]. During our research, polymerization temperature cycle for plastic scintillator manufacturing [9] and novel plastic scintillator with short rise and decay times for TOF-PET detectors [10] were developed.

In order to build the whole-body J-PET scanner with 200-cm length, we need plastic scintillators with low light attenuation characterized by a technical attenuation length (TAL) defined as the length of the scintillator reducing the light signal to 36.8% of its initial intensity [11]. The TAL value depends on bulk transmission of the scintillator, shape and thickness of the scintillator, reflective properties of the scintillator's surfaces, and foils' reflectivity, if they are used. The bigger the TAL value is, the higher the number of photons propagating along the scintillator strip, reaching silicon photomultipliers at both ends and increasing time and energy resolution of the J-PET scanner.

Similar parameter describing the scintillator's transparency is the bulk attenuation length (BAL) which depends on bulk transmission of the scintillator volume only and is not affected by scintillator shape, thickness, and loss of light on its surfaces during many total internal reflections. BAL is often present in manufacturers' specifications but TAL is a more useful property of scintillators in view of radiation detectors construction. TAL includes all the mentioned factors and thus it is lower than BAL.

In addition, it is important to stress that the light attenuation depends on the wavelength of the emitted photons [12].

TABLE I

PROPERTIES OF PLASTIC SCINTILLATORS USED IN THIS STUDY. ND, NO DATA AVAILABLE. DATA ARE TAKEN FROM MANUFACTURERS BROCHURES

Plastic scintillator type	Light output [% anthracene]	Decay time [ns]	Wavelength of maximum emission [nm]	Light attenuation length [cm]	Polymer base	Density [g/cm ³]
EJ-200	64	2.1	425	380	PVT	1.023
UPS-923A	56	3.3	418	400	PS	1.06
SP32	56	2.5	425	ND	PS	1.03
Epic	50-60	2.4	415	200	PS	1.05

The wavelength spectrum of the photons changes by propagating the scintillator toward the photodiode. A strong attenuation of the short wavelength part of the emission spectrum is observed, which is connected to a higher light absorption of the polymer base in that spectral region and well-known self-absorption effects [13].

The quality of surface polishing influences strongly the reflective property of the scintillator and may change the TAL value [14]. Both the wrapping method and reflector type affect, in particular, the performance of long plastic scintillators [15]. A tight wrapping of the scintillator makes optical contact with its surface and reduces the number of light photons reflected by total internal reflection inside the scintillator.

The scintillator thickness plays also an important role in light transport. In the case of optical scintillating fibers, an increase in fiber attenuation with decreasing core diameter was observed [16]. Surface scattering effects dominate in small-diameter fibers, which decreases the TAL. A similar dependence was also observed for plastic scintillator rods of BC-404 with square cross section [17]. In general, it can be observed that a higher cross section of the scintillator leads to a higher TAL value. Another example of the influence of scintillator thickness on the measured TAL is found in Saint-Gobain Organic Scintillation Materials and Assemblies brochure for 12-cm-wide and 200-cm-long BC-408 sheets: for 5-mm-thick scintillator TAL equals 190 cm, for 10-mm-thick TAL = 210 cm, for 20-mm-thick TAL = 275 cm, and BAL value from brochure is 380 cm.

The plastic scintillation material for TOF-PET systems must have a TAL at least of the same order as the length of the radiation detector. This means that the scintillator material used in the next whole-body J-PET prototype should be characterized by the TAL value of about 1000 mm or higher. A high TAL value will increase photon statistics and will provide a better position resolution along the strip. For the new J-PET prototype, we need a scintillator with short decay time (few nanoseconds) and wavelength of maximum emission close to maximum quantum efficiency of light detection of silicon photomultipliers for positron emission tomography (PET) application (450 nm).

TAL can be measured by irradiating the plastic scintillator by collimated radioactive source and signal readout by a photomultiplier [18] or by a lamp or diode with ultraviolet (UV) light emission and silicon photodiode signal readout [19]. In the first case, gamma radiation interacts with plastic scintillator volume via Compton scattering. Part of gamma quanta energy is deposited into the polymer matrix and it is converted

into blue light by dissolved fluorescent substances. The second method of excitation of the plastic scintillator is based on the direct illumination of the fluorescent substance by UV lamp or diode placed near scintillator surface. The emission spectrum of the UV lamp is overlapping with the absorption spectrum of fluorescent addition responsible for final blue light emission in the plastic scintillator. For both cases, blue light is finally emitted by fluorescent substance in the scintillator and transported with many total internal reflections to the light detector coupled at one end of the strip. The readout geometry and the light extraction cone can also influence the TAL value in the measurements. Different TAL values can be obtained by applying a few-millimeter air gap or optical grease between the photodetector and the scintillating fiber [20]. Using the UV diode and silicon photodiode is faster and more convenient for measurement of large amounts of scintillators and scintillating fibers and can be used for quality control during manufacturing of scintillators.

II. PERFORMED MEASUREMENTS

For a 1-m J-PET module, we choose to test four types of plastic scintillators from different manufacturers: EJ-200 from Eljen Technology [21], UPS-923A from Amcrys, Institute for Scintillation Materials [22], SP32 from Nuviotech Instruments [23], and the plastic scintillator from Epic-Crystal [24]. For each scintillator type, two scintillator pieces were tested. All four tested scintillator types have rectangular cross section and dimensions of 6 mm × 24 mm × 1000 mm with all surfaces polished. During TAL measurement, no reflecting foil was used.

All chosen scintillators have decay time in the range from 2.1 to 3.3 ns, wavelength of maximum emission from 415 to 425 nm, and light output between 50% and 64% of anthracene. The main selection criterion was a high light attenuation length value. For these four scintillators, light attenuation length values taken from manufacturer specifications were in the range 200–400 cm (see Table I). One scintillator (EJ-200) is made from polyvinyl toluene (PVT) as polymer base and three others are manufactured from polystyrene (PS).

The experimental setup for TAL measurement is presented in Fig. 1. The plastic scintillator strip is placed on a few plastic supports inside a light-tight aluminum rail with sliding lid at the top. The aluminum rail acts as a light-tight box shielding scintillator and photodetector from ambient light. The rail is painted in matte black that prevents scattered light reflections. In the sliding lid, 8-mm diameter holes are drilled every 50 mm for UV lamp tip. At one end of aluminum rail, a silicon

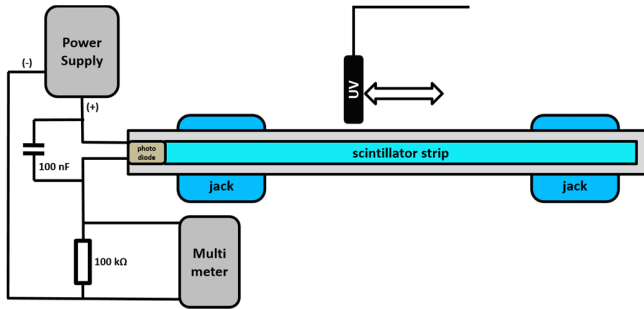


Fig. 1. Experimental setup for TAL measurements of 1-m plastic scintillators using a UV lamp and a photodiode.

photodiode with enhanced blue sensitivity Osram BPW 34B is mounted in plastic endcap and connected to a power supply and a multimeter. The silicon photodiode is attached at the center of the plastic scintillator end surface without optical gel or glue. The setup has additionally a 100-nF capacitor and a 100-k Ω resistor for readout stabilization. In this setup, the silicon photodiode is connected in reverse direction and the voltage drop across the 100-k Ω resistor measured by a digital multimeter Rigol DM3064, Rigol Technologies.

The idea of this measurement is based on excitation of the plastic scintillator by a UV lamp with 365-nm wavelength of maximum emission. The UV lamp is shining a few-millimeter spot on scintillator surface through a plastic tip inserted through a hole in the aluminum rail and the rest of the lamp is covered by a light-tight plastic tube. The plastic scintillator converts UV light to blue light which is emitted in all directions. Part of the blue light is reaching the silicon photodiode by total internal reflection inside the scintillator and is converted into electric pulses that are measured by the multimeter. The peak emission of the UV lamp at 365 nm is well matched with the absorption peak of the fluorescent substances used in blue-emitting plastic scintillators. For example, 1, 4-bis(5-phenyl-2-oxazolyl)benzene (POPOP) has absorption maximum at 358 nm and emission maximum at 425 nm [25]. In this measurement, only the fluorescent substance is excited which is responsible for the light emission in the studied plastic scintillator.

III. RESULTS

The results of the performed TAL measurement are presented in Fig. 2, showing the voltage measured by the photodiode as a function of the place of irradiation with the UV lamp. This voltage is proportional to the light intensity shining on the photodiode. The scintillators were excited along their length with 5-cm steps. Decrease of light intensity versus the UV lamp distance from the light detector can be characterized by the sum of two exponential functions:

$$I(x) = A_1 * e^{-\frac{x}{\lambda_S}} + A_2 * e^{-\frac{x}{\lambda_L}} + y_0 \quad (1)$$

where λ_S and λ_L are the short and long attenuation length components, respectively, A_1 and A_2 are amplitudes, and y_0 denotes the constant background. Equation (1) was fitted to measured data. Parameters of all the fits are gathered in Table II. Errors are calculated from the fit as standard deviation. Example of an overlap of the fit $I(x)$ with the data is presented in Fig. 2 (bottom).

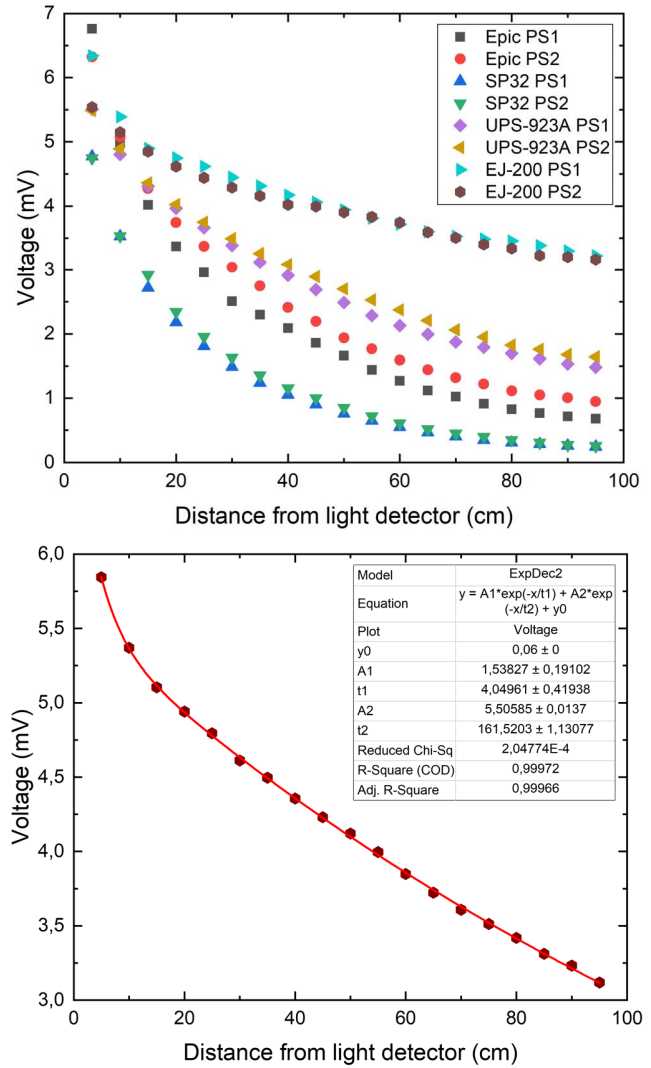


Fig. 2. (Top) Results of the TAL measurements for four types of commercially available plastic scintillators. Two strips of each type were tested. (Bottom) Example of an overlap of the fit $I(x)$ represented by the red line with the data (black points) for plastic scintillator EJ-200, strip PS1.

TABLE II

ATTENUATION PARAMETERS OBTAINED FROM FIT TO THE OBTAINED EXPERIMENTAL DATA. MEASURED TAL IS REPRESENTED BY λ_L . PS1 AND PS2 DENOTE TWO DIFFERENT STRIPS OF THE SAME PLASTIC SCINTILLATOR TYPE

Plastic scintillator strip	λ_S [cm]	λ_L [cm]	Value from specification [cm]
EJ-200 PS1	4.05 ± 0.42	161.5 ± 1.1	380
EJ-200 PS2	1.08 ± 0.05	166.9 ± 1.7	
UPS-923A PS1	4.06 ± 1.1	63.8 ± 0.58	400
UPS-923A PS2	4.17 ± 1.4	68.8 ± 0.61	
SP32 PS1	7.50 ± 0.69	28.3 ± 0.56	ND
SP32 PS2	7.16 ± 0.49	29.0 ± 0.41	
Epic PS1	6.27 ± 0.86	41.0 ± 0.67	200
Epic PS2	5.16 ± 0.33	49.4 ± 2.3	

The long attenuation length component, λ_L , is the TAL value, while the short one, λ_S , represents highly attenuated part of the emission spectrum. This short component is connected with self-absorption of blue-emitting fluorescent substance (WLS) where part of the absorption spectrum is overlapped

with emission spectrum. Part of the emission spectrum with shorter wavelength is more attenuated, for example, if scintillator has a maximum of emission at 425 nm and then part of the spectrum below 425 nm is rapidly attenuated and part above 425 nm up to 500 nm is less attenuated. Short attenuation length component depends on the concentration and type of fluorescent substance and polymer purity. The long attenuation length component λ_L represents remaining light that was not attenuated by self-absorption of WLS. This part of light propagates through the scintillator and is absorbed by the polymer, fluorescent substances, impurities, and scatters on surfaces during total internal reflections.

TAL values found in this research are smaller than the maximum values from manufacturers' data sheets. Big differences between measured and theoretical TAL values are caused mainly by different size of scintillators measured in our test and in producer's measurement. High TAL values are obtained usually for a few centimeters thick plastic scintillator sheets or blocks. For example, UPS-923A plastic scintillator with dimensions 20 mm \times 300 mm \times 2000 mm was characterized with a TAL value of 130 cm and a BAL value of 260 cm [11]. In our case, we have strips with small cross section 6 mm \times 24 mm and light is more attenuated in such smaller scintillators. In thinner scintillators, light undergoes more internal reflections compared to thicker scintillators with the same length. Each additional reflection on the scintillator surface increases the light loss due to scratches and patterns caused by the polishing machine.

IV. CONCLUSION

EJ-200 possesses the best properties regarding light attenuation with TAL over 160 cm. This low attenuation allows us to build total-body J-PET prototype from 2-m scintillator strips or combination of 1-m strips forming diagnostic chamber for simultaneous whole body imaging.

Three PS-based plastic scintillators have smaller TAL values. Polymer matrix should not be the reason for the higher light attenuation because both polymers, polyvinyltoluene and PS, are amorphous and they are very transparent to visible light. Scintillating fibers are produced from PS with a few meters TAL. Probably, the reasons for the big differences in transparency of tested scintillators are method of monomer and fluorescent additions purification, type and concentration of fluorescent substances, polymerization conditions, and surface polishing techniques used by the companies.

ACKNOWLEDGMENT

The author acknowledges the technical and administrative support of A. Heczko, M. Kajetanowicz, and W. Migdał.

REFERENCES

- [1] P. Moskal *et al.*, "Test of a single module of the J-PET scanner based on plastic scintillators," *Nucl. Instrum. Meth. Phys. Res. A, Accel. Spectrom. Detect. Assoc. Equip.*, vol. 764, pp. 317–321, Nov. 2014.
- [2] S. Niedzwiecki, "J-PET: A new technology for the whole-body PET imaging," *Acta Physica Polonica B*, vol. 48, pp. 1567–1576, Oct. 2017.
- [3] P. Moskal *et al.*, "Time resolution of the plastic scintillator strips with matrix photomultiplier readout for J-PET tomograph," *Phys. Med. Biol.*, vol. 61, no. 5, pp. 2025–2047, Feb. 2016.
- [4] J. Smyrski *et al.*, "Measurement of gamma quantum interaction point in plastic scintillator with WLS strips," *Nucl. Instrum. Meth. Phys. Res. A, Accel. Spectrom. Detect. Assoc. Equip.*, vol. 851, pp. 39–42, Apr. 2017.
- [5] P. Kowalski *et al.*, "Estimating the NEMA characteristics of the J-PET tomograph using the GATE package," *Phys. Med. Biol.*, vol. 63, no. 16, pp. 165008-1–165008-17, Aug. 2018.
- [6] P. Moskal *et al.*, "Feasibility study of the positronium imaging with the J-PET tomograph," *Phys. Med. Biol.*, vol. 64, no. 5, pp. 055017-1–055017-14, Mar. 2019.
- [7] P. Moskal, B. Jasińska, E. L. Stępień, and S. D. Bass, "Positronium in medicine and biology," *Nature Rev. Phys.*, vol. 1, no. 9, pp. 527–529, Jun. 2019.
- [8] G. Korcyl *et al.*, "Evaluation of single-chip, real-time tomographic data processing on FPGA SoC devices," *IEEE Trans. Med. Imag.*, vol. 31, no. 11, pp. 2526–2535, Nov. 2018.
- [9] L. Kapton *et al.*, "Plastic scintillators for positron emission tomography obtained by the bulk polymerization method," *Bio-Algorithms Med.-Syst.*, vol. 10, no. 1, pp. 27–31, Jan. 2014.
- [10] A. Wieczorek *et al.*, "Novel scintillating material 2-(4-styrylphenyl)benzoxazole for the fully digital and MRI compatible J-PET tomograph based on plastic scintillators," *PLoS ONE*, vol. 12, no. 11, pp. e018672-1–e018672-16, Nov. 2017.
- [11] A. Artikov *et al.*, "Properties of the Ukraine polystyrene-based plastic scintillator UPS 923 A," *Nucl. Instrum. Meth. Phys. Res. A, Accel. Spectrom. Detect. Assoc. Equip.*, vol. 555, nos. 1–2, pp. 125–131, Dec. 2005.
- [12] V. Senchyshyn, V. Lebedev, A. Adadurov, J. Budagov, and I. Chirikov-Zorin, "Accounting for self-absorption in calculation of light collection in plastic scintillators," *Nucl. Instrum. Meth. Phys. Res. A, Accel. Spectrom. Detect. Assoc. Equip.*, vol. 566, no. 2, pp. 286–293, Oct. 2006.
- [13] P. Rebourgeard *et al.*, "Fabrication and measurements of plastic scintillating fibers," *Nucl. Instrum. Meth. Phys. Res. A, Accel. Spectrom. Detect. Assoc. Equip.*, vol. 427, no. 3, pp. 543–567, May 1999.
- [14] M. Gierlik, T. Batsch, R. Marcinkowski, M. Moszyński, and T. Sworobowicz, "Light transport in long, plastic scintillators," *Nucl. Instrum. Meth. Phys. Res. A, Accel. Spectrom. Detect. Assoc. Equip.*, vol. 593, no. 3, pp. 426–430, Aug. 2008.
- [15] A. Taheri and R. G. Peyvandi, "The impact of wrapping method and reflector type on the performance of rod plastic scintillators," *Measurement*, vol. 97, pp. 100–110, Feb. 2017.
- [16] C. Whittaker, C. A. G. Kalnins, D. Ottaway, N. A. Spooner, and H. Ebendorff-Heidepriem, "Transmission loss measurements of plastic scintillating optical fibres," *Opt. Mater. Express*, vol. 9, no. 1, pp. 1–12, Jan. 2019.
- [17] M. Kurata *et al.*, "Study of timing degradation and light attenuation in long plastic scintillation rods for time-of-flight counters in relativistic heavy ion experiments," *Nucl. Instrum. Meth. Phys. Res. A, Accel. Spectrom. Detect. Assoc. Equip.*, vol. 349, nos. 2–3, pp. 447–453, Oct. 1994.
- [18] A. E. Baulin *et al.*, "Attenuation length and spectral response of kuraray SCSF-78MJ scintillating fibres," *Nucl. Instrum. Meth. Phys. Res. A, Accel. Spectrom. Detect. Assoc. Equip.*, vol. 715, pp. 48–55, Jul. 2013.
- [19] A. B. R. Cavalcante *et al.*, "Refining and testing 12,000 km of scintillating plastic fibre for the LHCb SciFi tracker," *J. Instrum.*, vol. 13, no. 10, pp. P10025-1–P10025-22, Oct. 2018.
- [20] K. Pauwels *et al.*, "Single crystalline LuAG fibers for homogeneous dual-readout calorimeters," *J. Instrum.*, vol. 8, no. 9, pp. P09019-1–P09019-16, Sep. 2013.
- [21] Eljen Technology, USA. *EJ-200 Plastic Scintillator*. Accessed: Nov. 4, 2019. [Online]. Available: <https://eljentechnology.com/products/plastic-scintillators/ej-200-ej-204-ej-208-ej-212>
- [22] Institute for Scintillation Materials, Ukraine. *UPS-923A Plastic Scintillator*. Amcrys. Accessed: Nov. 4, 2019. [Online]. Available: http://www.amcrys.com/details.html?cat_id=146&id=4286
- [23] Nuviattech Instruments, Czechia. *SP32 Plastic Scintillator*. Accessed: Nov. 4, 2019. [Online]. Available: <http://www.nuviattech-instruments.com/product/nudet-plastic/>
- [24] Epic-Crystal, China. *Plastic Scintillator*. Accessed: Nov. 4, 2019. [Online]. Available: <http://www.epic-crystal.com/others/plastic-scintillator.html>
- [25] U. Brackmann, *Lambdachrome Laser Dyes*, 3rd ed. Göttingen, Germany: Lambda Physik AG, 2000.